View metadata, citation and similar papers at core.ac.uk

brought to you by CORE

provided by Open Archive Toulouse Archive Ouverte

Open Archive Toulouse Archive Ouverte (OATAO)

OATAO is an open access repository that collects the work of Toulouse researchers and makes it freely available over the web where possible.

This is an author-deposited version published in: http://oatao.univ-toulouse.fr/
Eprints ID : 2440

To link to this article :
URL : http://dx.doi.org/10.1016/j.tsf.2007.04.007

To cite this version : Maury, Francis and Duminica, F.-D (2007) *Diagnostic in TCOs CVD processes by IR pyrometry.* Thin Solid Films, vol. 515 (n° 24). pp. 8619-8623. ISSN 0040-6090

Any correspondence concerning this service should be sent to the repository administrator: staff-oatao@inp-toulouse.fr

Diagnostic in TCOs CVD processes by IR pyrometry

F. Maury *, F.-D. Duminica

CIRIMAT, CNRS/INPT/UPS, ENSIACET, 118 Route de Narbonne, 31077 Toulouse cedex 4, France

Abstract

Infra red pyrometry is a sensitive, simple and low-cost technique commonly used for the measurement of the deposition temperature in CVD processes. We demonstrate in this work that this optical technique can be used as diagnostic tool to provide fruitful informations during the growth under atmospheric pressure of TiO_2 films on various substrates chosen as an example of transparent oxide. Significant variations of the pyrometric signal were observed during the deposition of TiO_2 thin films due to interferences in the growing film resulting from multi-reflections at the interfaces and scattering induced by the surface roughness. Modeling of the time dependence of the IR pyrometric signal allows simultaneously the determination of the layer thickness, the growth rate, surface roughness and refractive index of the thin films under the growth conditions. This diagnostic technique can be used for various transparent thin films grown on opaque substrates and is well adapted to control CVD processes operating either under atmospheric or low pressure and more generally any thermal treatment processes.

Keywords: IR pyrometry; *In situ* analysis; Diagnostic tool; TiO_2 thin films; Transparent films; CVD

1. Introduction

Titanium dioxide films have been extensively investigated for many applications. For instance, they are used as antireflective layers for optical devices [1,2], as photo-catalysts for the decontamination and purification of environmental pollutants [3,4] and as super-hydrophilic thin layers for self-cleaning surfaces [5]. Among the TiO_2 growth processes, atmospheric pressure metal organic chemical vapor deposition (MOCVD) is a promising technique because no vacuum system is required and it is known for its good capability for large-scale production and uniform coverage [6]. Additionally, it is a suitable process for continuous deposition. However, an industrial production requires an optimization and a good control of the growth process.

This can be achieved using surface diagnostic tools. For instance, *in situ* analysis of the dynamic of the growth and, subsequently, real time control of the growth rate was reported using techniques operating under vacuum environment such as reflection high energy electron diffraction (RHEED) [7] and near-threshold photoemission [8]. For diagnostic and *in situ* monitoring of atmospheric deposition processes, the optical techniques are more appropriate. However, they are generally complex in terms of equipment and analysis of the data, as for instance reflectance difference spectroscopy (RDS) [9], surface photo-absorption (SPA) [10] and surface photo-interference (SPI) [11]. Fast spectroscopic ellipsometers [12] and laser interferometry [13] can provide direct real time informations on the optical parameters and thickness of a growing film. However, these instruments are relatively expensive. Furthermore, they exhibit a low flexibility and frequently require specific reactor design.

IR pyrometry is a classical technique for the temperature measurement. It is less known that it can be used also as a surface diagnostic tool to control the growth of a large variety of thin film materials that exhibits an emissivity sufficiently different from that of the substrate. A monochromatic radiation pyrometer measures the intensity of the light emitted by a body at a given wavelength with a high sensitivity. *In situ* IR pyrometry has been used for real time monitoring of the early stages of the MOCVD growth of metal-like CrC_xN_y thin films. Changes of emissivity of the film/substrate couples were correlated to the growth rate of the film [14]. When a film is transparent to the emitted radiation the determination of the true temperature of a film/substrate system is sometime complicated by oscillations due to interference effects originating from multireflections at the interfaces [15]. Interestingly, pyrometric interferometry was used in a microwave plasma-assisted CVD process for *in situ* control of the growth rate of diamond thin

* Corresponding author. Tel.: +33 562885669; fax: +33 562885600.
E-mail address: francis.maury@ensiacet.fr (F. Maury).

doi:10.1016/j.tsf.2007.04.007

film, which is transparent to the radiation detected by the pyrometer [16,17]. This method was also used during MBE growth of partially opaque layers of III–V semiconductors [18] and device heterostructures [19].

We demonstrate in this paper that IR pyrometry is an attractive diagnostic tool for a large variety of vapor phase deposition processes to provide real time informations on the growth of various thin film materials. Indeed, in addition to the above cited references, the technique has been applied successfully during the growth under atmospheric pressure of TiO_2 on various opaque substrates including silicon and steel using different CVD processes. The optical constants and the growth rate of the TiO_2 films were *in situ* determined. Perspectives and capabilities of the method are discussed.

2. Theory and methodology

The optical pyrometer measures the spectral luminance of a real body according to the equation:

$$L_{\lambda,T} = \varepsilon_\lambda L^{bb}_{\lambda,T} \tag{1}$$

where, ε_λ is the spectral emissivity of the radiating body and $L^{bb}_{\lambda,T}$ is the spectral luminance of the black body. Both parameters depend on the wavelength λ. The spectral luminance of the black body depends on the temperature according to the Planck's law which can be approximated by the Wien's law when $hc/\lambda \gg k_B T$:

$$L^{bb}_{\lambda,T} = \frac{2\pi hc^2\lambda^{-5}}{\exp\left(\frac{hc}{\lambda k_B T}\right)} \tag{2}$$

where k_B is the Boltzmann constant, h is the Planck constant and c is the speed of the light under vacuum. The spectral emissivity ε_λ depends on the reflectivity and transmittance of the material and depends also on its surface roughness (σ). Generally, the highest values of emissivity are obtained for the roughest surfaces.

Before the growth of the film, the pyrometric signal corresponds to the radiation emitted by the substrate (combining Eqs. (1) and (2)):

$$L^{subs}_{\lambda,T} = \varepsilon^{subs}_{\lambda,T}\cdot L^{bb}_{\lambda,T} = \frac{2\pi hc^2\varepsilon_{subs}(\lambda,T)}{\lambda^5}\exp\left(-\frac{hc}{k_B T\lambda}\right) \tag{3}$$

When the deposited film exhibits an emissivity significantly different from that of the substrate, and for a given temperature, if the spectral emissivity is fixed on the pyrometer at the value of the substrate, then the apparent temperature (or pyrometric signal) will significantly change according to the above equations.

In the particular case of a transparent thin film deposited on a substrate, Yin et al. [16] have considered that spectral luminance of the film/substrate system is essentially the radiation transmitted by the substrate through the transparent film:

$$L^{film/subs}_{\lambda,T} = T^{film}_{\lambda,T,\sigma}\cdot L^{bb}_{\lambda,T} \tag{4}$$

where $T^{film}_{\lambda,T,\sigma}$ is the transmittance of the film.

As we will see in Section 4, the Yin's model presents a satisfying agreement with the experimental data at the beginning of the growth, but the discrepancy between the experimental data and the Yin's model increases with the deposition time, *i.e.* with the thickness of the film. In fact, the Yin's model neglects the absorption effects in the growing film. We suppose that the discrepancy is due to the emissivity of the growing film, which is negligible at the beginning of the growth, and the contribution of which increases with the film thickness.

In an analogous way to the Yin's model, for a semi-transparent film as a relatively thick TiO_2 film, the spectral luminance of the film/substrate system can be considered as the sum between the substrate radiation contribution through the semi-transparent film [14] and the intrinsic spectral luminance of the growing film:

$$\begin{aligned} L^{film/subs}_{\lambda,T} &= (\varepsilon^{subs}_{\lambda,T}\cdot T^{film}_{\lambda,T,\sigma} + \varepsilon^{film}_{\lambda,T,\sigma})L^{bb}_{\lambda,T} \\ &= \frac{2\pi hc^2(\varepsilon^{subs}_{\lambda,T}\cdot T^{film}_{\lambda,T,\sigma} + \varepsilon^{film}_{\lambda,T,\sigma})}{\lambda^5}\exp\left(-\frac{hc}{k_B T_{app}\lambda}\right) \end{aligned} \tag{5}$$

As for the Yin's model, this last equation of the modified model serves as the definition of the apparent temperature T_{app} (*i.e.* the pyrometric signal).

The value of the apparent temperature can be determined from Eqs. (3) and (5):

$$T_{app} = \frac{T}{1 + \frac{T}{\frac{hc}{k_B\lambda}}\ln\left[T^{film}_{\lambda,T,\sigma} + \frac{\varepsilon^{film}_{\lambda,T,\sigma}}{\varepsilon^{subs}_{\lambda,T}}\right]} \tag{6}$$

Considering that a body can emit (ε) what it can absorb, the spectral emissivity of the film was calculated using the formula [17,20]:

$$\varepsilon^{film}_{\lambda,T,\sigma} = 1 - \exp\left(\frac{4\pi k_{film} d}{\lambda}\right) \tag{7}$$

where, k_{film} is the extinction coefficient of the film.

The transmittance of the growing film $T^{film}_{\lambda,d,\sigma}$ depends on the wavelength (λ) as well as on the thickness (d) and the roughness of the film (σ). The surface roughness of TiO_2 layers causes radiation losses by scattering, which reduces the transmittance of the layer (Fig. 1). In order to take into account the effect of the surface roughness on the optical properties, the model proposed by Filinski has been used [21]. The reflection and the transmission of a beam emitted by a substrate through a film have been previously described [22]. The scattering factors S_{int} and S_t for a film surface with root mean square roughness σ are given by [22]:

$S_{int10} = \exp[-1/2(4\pi\sigma_{film}n_1/\lambda)^2]$ correlated with the reflection inside the film from the external surface;
$S_{int12} = \exp[-1/2(4\pi\sigma_{subs}n_1/\lambda)^2]$ correlated with the reflection inside the film from substrate;
$S_{t21} = \exp[-1/2(2\pi\sigma_{subs}(n_2 - n_1)/\lambda)^2]$ correlated with the transmission from the substrate to the film;
$S_{t10} = \exp[-1/2(2\pi\sigma_{film}(n - n_0)/\lambda)^2]$ correlated with the transmission from the film to the surface;where: n_0, n_1 and

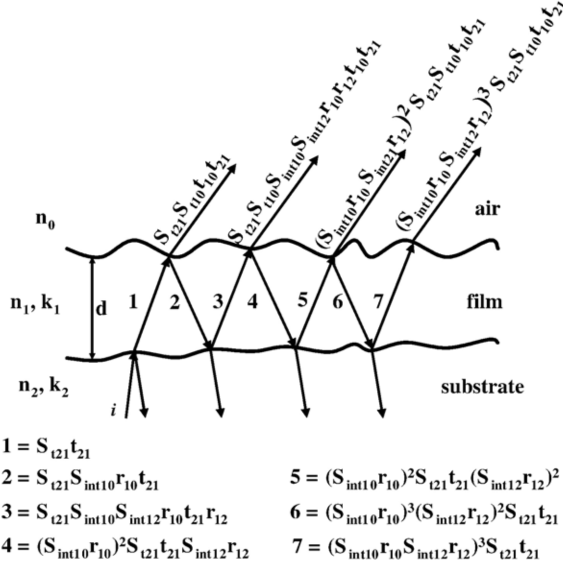

Fig. 1. Schematic diagram of a film/substrate system showing that the light emitted by the substrate undergoes interferences in the growing film and scattering from the surface roughness of the film.

n_2 are the real refractive indexes of the air, the film and the substrate, respectively, σ_{film} and σ_{subs} are the roughness of the film and the substrate (Fig. 1).

The transmittance from the rough growth surface of the film is given by [20,22]:

$$T_{\text{film}} = \frac{n_2}{n_0} \cdot \frac{[(1+g_1)^2 + h_1^2][(1+g_2)^2 + h_2^2]S_{t21}^2 S_{t10}^2}{\beta + S_{\text{int}10}^2 S_{\text{int}12}^2 (g_1^2 + h_1^2)(g_2^2 + h_2^2)\beta^{-1} + S_{\text{int}10} S_{\text{int}12}(A\cos 2\gamma_1 + B\sin 2\gamma_1)} \tag{8}$$

where:

$$g_1 = \frac{n_0^2 - n_1^2 - k_1^2}{(n_0 + n_1)^2 + k_1^2} \quad g_2 = \frac{n_1^2 - n_2^2 + k_1^2 - k_2^2}{(n_1 + n_2)^2 + (k_1 + k_2)^2} \quad A = -2(g_1 g_2 - h_1 h_2)$$

$$h_1 = \frac{2 n_0 k_1}{(n_0 + n_1)^2 + k_1^2} \quad h_2 = \frac{2(n_1 k_2 - n_2 k_1)}{(n_1 + n_2)^2 + (k_1 + k_2)^2} \quad B = -2(g_1 h_2 + h_1 g_2)$$

$$\gamma = \frac{2\pi n_1 d}{\lambda} \qquad \beta = \exp\left(\frac{4\pi k_1 d}{\lambda}\right)$$

By substituting the expression of the transmittance given by Eq. (8) in the Eq. (6), the variation of the apparent temperature *versus* the deposition time can be deduced.

At this stage, we are interested by the temporal dependence of the pyrometric signal during the growth with the aim to obtain a mean growth rate. The thickness of the film is supposed to depend directly on the deposition time (t) and the average growth rate of the layer (G). The growth rate of the film, $G = d/t$, can be determined *in situ* from the oscillation period (P) of the pyrometric signal using the equation deduced by Thorpe [19]:

$$G = \frac{\lambda}{2 \cdot n \cdot P} \tag{9}$$

In addition, the simulation of the temporal variation of the pyrometric signal based on the combination of Eqs. (6) and (8) is possible, but some assumptions used in this model have to be kept in mind. In particular, it is assumed that the composition and subsequently the intrinsic optical properties, as well as the growth rate of the film remain constant in the course of time. About the film roughness, we supposed in our calculations a linear variation of the roughness *versus* the deposition time. Despite these assumptions, this model (Eq. (6)) gives a good agreement of the temporal dependence of the pyrometric signal in the case of TiO_2 films grown on Si and steel as demonstrated in the next sections.

3. Experimental

The TiO_2 layers were grown by two different CVD processes using a vertical cold-wall reactor similar to the one previously described [6]. The two processes were chosen because they provide TiO_2 films with significantly different features. Here it suffices to identify them as processes 1 and 2. The experimental set-up for *in situ* IR pyrometric analysis was described elsewhere [14]. The temperature of the substrate was measured using a thermocouple inserted in the sample holder. This experimental value is considered as the true temperature.

A monochromatic ($\lambda = 1.6$ μm) IR pyrometer (AOIP model TR7020E) was used to measure the radiation emitted by the heated samples. The sample surface was aimed through the quartz wall of the reactor with an incidence of approximately 30° to the normal of the surface. The pyrometric data *versus* time were collected with a computer. If the total emissivity of the film/substrate system was known, the temperature could be determined from the pyrometric signal. The spectral emissivity depends on the material and, generally, metals exhibit lower values than oxides and silicon. Depending on the substrate, the emissivity coefficient was fixed on the pyrometer to the value of Si ($\varepsilon_{\text{Si}} = 0.68$) or steel ($\varepsilon_{\text{Fe}} = 0.25$). As a result, the pyrometric signal is sensitive to changes of emissivity during the deposition and the measured value corresponds to an apparent temperature.

4. Results and discussion

TiO_2 thin films are uniformly deposited on various substrates with different bright colors depending on their thickness

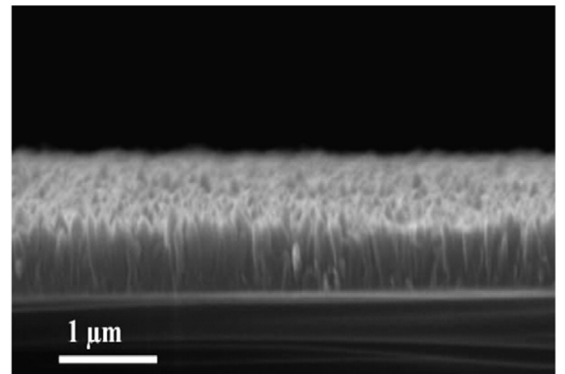

Fig. 2. SEM micrographs showing the typical columnar structure of the TiO_2 layers grown by atmospheric pressure CVD (process 1).

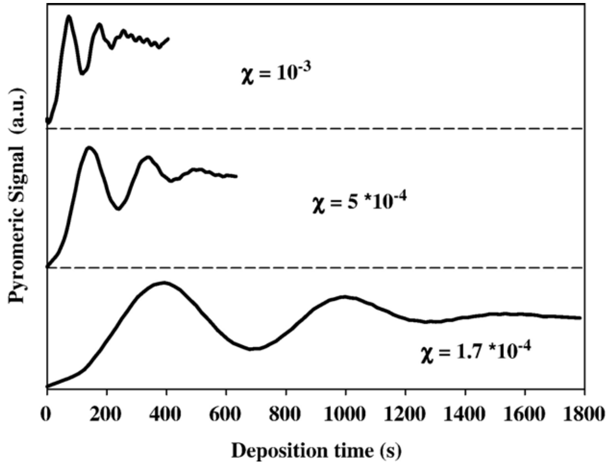

Fig. 3. Variation of the pyrometric signal with the deposition time during three TiO_2 CVD runs carried out at 500 °C on Si(100) using different mole fractions of the Ti molecular precursor: 170, 500 and 1000 ppm (process 1).

(interferential colors). The two types of CVD processes lead to different characteristics of the TiO_2 layers whatever the substrates.

Fig. 2 shows a typical SEM micrograph of the surface and cross section of a film deposited by the process 1. The film exhibits a columnar and porous structure with a rough surface morphology constituted of sharp protruding uniform columns.

Fig. 3 shows the typical variation of the pyrometric signal with the deposition time of three TiO_2 films carried out during the process 1 at 500 °C using different mole fractions of the titanium molecular precursor: 170, 500 and 1000 ppm. The increase of Ti precursor mole fraction induces a reduction of the oscillation period of the pyrometric signal. We also know that in this process the growth rate increases with the mole fraction of the Ti source [6]. As a result, this indicates that the oscillation period decreases by increasing the growth rate. This is in good agreement with Eq. (9) which indicates that the growth rate is inversely proportional to the oscillation period.

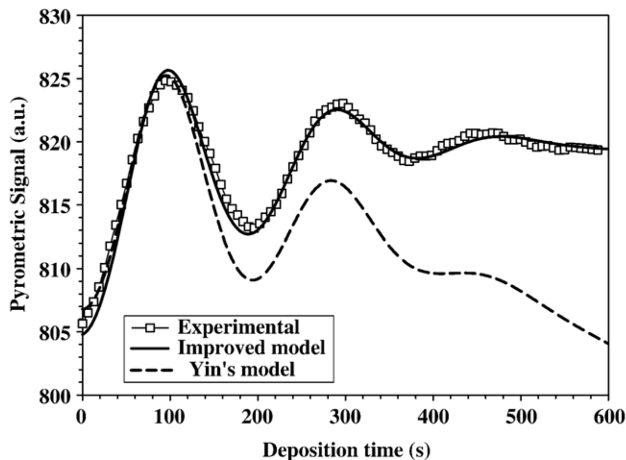

Fig. 4. Experimental and theoretical variations of the pyrometric signal with the deposition time for a TiO_2 CVD run carried out on Si(100) at 550 °C. The parameters provided by the improved model are: $G=2.7$ nm/s; $n_{film}=1.45$; $k_{film}=0.015$; σ (nm)$=0.4\cdot$time (s); thickness$=1620$ nm (thickness measured by SEM$=1600$ nm).

Fig. 4 shows a comparison between the experimental pyrometric signal and the two models described above: the Yin's model (dotted line) and the improved model corresponding to the Eq. (6) (full line). The amended model fits quite well the experimental data. The experimental growth conditions are reported in the legend of Fig. 4, as well as the parameters provided by the improved model: growth rate, optical constants and film roughness.

It is noteworthy that the film thickness determined *in situ* by this method (1620 nm) is in very good agreement with the value measured by SEM (1600 nm). Furthermore, the roughness of the substrate was considered negligible ($\sigma_{subs}=0$ for $t=0$) and the surface roughness of the film measured after the CVD run by optical interferometry was 200 nm, while the calculated roughness using the model was 240 nm. This experiment performed on the very smooth (100) surface of a single-crystalline Si wafer validates the model. The experimental value of the refractive index measured at 25 °C by ellipsometry was $n=1.73$ and $k=0.004$ (for $\lambda=1.5$ μm). The lower value of the film index n compared to bulk TiO_2 is explained by the porosity of the film. However this is the same order of magnitude than the values deduced from the model. Compared to *ex situ* measurement at 25 °C by ellipsometry, the lower value of refractive index n measured *in situ* by IR pyrometry ($n=1.45$, $k=0.015$) is explained by the fact that the *in situ* measurement was performed at the deposition temperature (550 °C) rather than room temperature and it is known that the refractive index decreases as the temperature increases with a thermo-optic coefficient of $3\cdot10^{-4}$ K^{-1} at 800 nm for temperature range 220–325 °C [23]. Furthermore, measurement was performed at $\lambda=1.5$ μm by ellipsometry, and 1.6 μm by *in situ* IR pyrometry.

IR pyrometry and the improved model described above have also been applied to TiO_2 layers deposited on the same substrates using another process (process 2). Under these conditions, TiO_2 films are particularly uniform and denser on both substrates compared with CVD layers grown by process 1 as shown in Fig. 5. Fig. 6 shows the temporal variation of the experimental and calculated pyrometric signals by using the improved model during the growth of TiO_2 compact layer

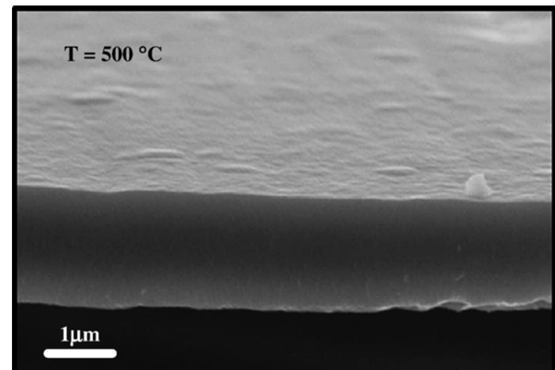

Fig. 5. SEM micrograph showing the smooth and compact morphology of a TiO_2 layer grown at 500 °C by the process 2 (cross section of a thick flake detached from a steel coupon).

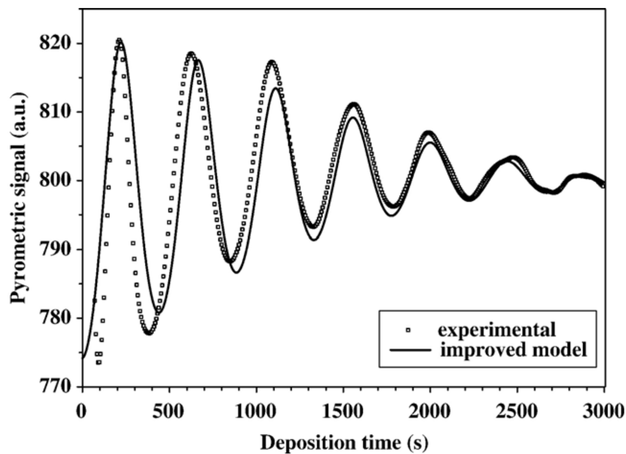

Fig. 6. Experimental (doted line) and theoretical variations (full line) of the pyrometric signal with the deposition time for a compact TiO_2 layer grown at 500 °C by the process 2 on steel. The parameters provided by the model are: G=0.92 nm/s; n_{film}=1.97; k_{film}=0.0013; σ_{film} (nm)=0.035·time (s)+σ_{subs} (40 nm); thickness=2760 nm (thickness measured by SEM=2800 nm).

(process 2). In the example shown, the substrate was a polished steel coupon ($\sigma_{subs}\sim 40$ nm for $t=0$). The surface roughness of the film measured after the CVD run by optical interferometry was 120 nm, while the calculated roughness using the model was 165 nm (σ_{film} (nm)=0.035·time (s)+σ_{subs}). The experimental growth conditions and the data provided by the model are given in the legend of Fig. 6. The experimental value of the refractive index measured at 25 °C by ellipsometry was $n=2.43$ and $k=0.0009$ (for $\lambda=1.5$ μm), while the calculated refractive index measured *in situ* by IR pyrometry were $n=1.97$ and $k=0.0013$). These values are in satisfactory agreement with literature data, $n=1.99$–2.44 and $k=2.7$–$9\cdot 10^{-3}$ [23]. Compared to the CVD TiO_2 film from process 1, the higher value of the refractive index of this compact film (process 2) is in agreement with its lower porosity as evidenced by SEM micrographs (Figs. 2 and 5). A good fitting was obtained between the experimental and calculated curves. As a result, a good agreement was found for the growth rate measured *in situ* by IR pyrometry (2760 nm) and by SEM (2800 nm). The amplitude and the number of oscillations observed for TiO_2 films grown by the process 2 are higher than those observed for process 1. This is explained on one hand by the difference of film porosity which depends on the growth process (lower the porosity, higher the amplitude) and, on the other hand, by the higher difference of spectral emissivity between the substrate and the film which are different for the two examples shown.

5. Conclusions

Significant variations of the pyrometric signal were observed during the growth of TiO_2 by different CVD processes on various substrates. The emissivity depends on the nature, the thickness and the roughness of the films. The radiation of the film/substrate system detected by IR pyrometry originates essentially from the substrate by transmission through the transparent film. As a result, oscillations due to multireflections were observed. A model based on emissivity and the interferences between the substrate and the growing layer was proposed to explain the oscillations of the pyrometric signal in the early stages of the growth. The deposition rate can be determined *in situ* using this model in addition to the optical indexes and the roughness of film.

In addition to the temperature measurement, which is its first functionality, optical pyrometry is a very attractive diagnostic tool for real time monitoring of CVD processes. It can be used for *in situ* control of the growth, even under atmospheric pressure, of a large variety of thin films, especially transparent oxide films. Indeed, the technique has been successfully used in our Laboratory to study the growth of TiO_2, SnO_2, nitrides and oxynitrides thin films and it offers good perspectives for other materials. It is a sensitive, simple and low-cost technique that is, as an additional advantage, easy to adapt on conventional CVD reactors and related vapor deposition processes.

References

[1] C. Martinet, V. Paillard, A. Gagnaire, J. Joseph, J. Non-Cryst. Solids 216 (1997) 77.
[2] M.G. Kang, N.-G. Park, Y.J. Park, K.S. Ryu, S.H. Chang, Sol. Energy Mater. Sol. Cells 75 (2003) 475.
[3] I.K. Konstantinou, T.A. Albanis, Appl. Catal., B Environ. 42 (2003) 319.
[4] D. Robert, A. Piscopo, O. Heintz, J.V. Weber, Catal. Today 54 (1999) 291.
[5] M. Kamei, T. Mitsuhashi, Surf. Sci. 463 (2000) L609.
[6] F.-D. Duminica, F. Maury, F. Senocq, Surf. Coat. Technol. 188–189 (2004) 255.
[7] J. Zhang, A.G. Taylor, J.M. Fernandez, B.A. Joyce, A.R. Turner, M.E. Pemble, J. Cryst. Growth 150 (1995) 1015.
[8] N. Viguier, F. Maury, Appl. Phys. Lett. 74 (1999) 266.
[9] K. Ploska, J.T. Zettler, W. Richter, J. Jonsson, F. Reinhardt, J. Rumberg, M. Pristovsek, M. Zorn, D. Westwood, R.H. Williams, J. Cryst. Growth 145 (1994) 44.
[10] R.F. Yates, H.M. Yates, M.E. Pemble, J. Cryst. Growth 195 (1998) 174.
[11] A. Yoshikawa, M. Kobayashi, S. Tokita, J. Cryst. Growth 145 (1994) 68.
[12] Y. Leprince-Wang, K. Yu-Zhang, V. Nguyen Van, D. Souche, J. Rivory, Thin Solid Films 307 (1997) 38.
[13] M.E. Pemble, in: M.D. Allendorf, F. Maury, F. Teyssandier (Eds.), Chem. Vap. Deposition XVI, EUROCVD 14, Electrochem. Soc., Pennington, NJ, Electrochem. Soc. Proc. Volume, PV 2003-08, 2003, p. 439.
[14] C. Gasquères, F. Maury, F. Ossola, Chem. vap. depos. 9 (2003) 34.
[15] G. Llauro, D. Hernandez, F. Sibieude, J.M. Gineste, R. Verges, D. Antoine, Appl. Surf. Sci. 135 (1998) 91.
[16] Z. Yin, Z.L. Akkerman, F.W. Smith, R. Gat, Mater. Res. Soc. Symp. Proc. 441 (1997) 653.
[17] S. Barrat, P. Pigeat, I. Dieduez, E. Bauer-Grosse, B. Weber, Thin Solid Films 263 (1995) 127.
[18] K. Biermann, A. Hase, H. Kunzel, J. Cryst. Growth 210-202 (1999) 36.
[19] A.J. Spring Thorpe, T.P. Humphreys, A. Majeed, W.T. Moore, Appl. Phys. Lett. 55 (1989) 2138.
[20] O.S. Heavens, Optical Properties of Thin Solid Films, Butterworths Scientific Publications, London, 1955, p. 76.
[21] I. Filinski, Phys. Status Solidi 49 (1972) 577.
[22] Z. Yin, H.S. Tan, F.W. Smith, Diamond Rel. Mater. 5 (1996) 1490.
[23] G. Gulsen, M. Naci Inci, Opt. Mater. 18 (2002) 373.